CHEMISTRY
A EUROPEAN JOURNAL

DOI: 10.1002/chem.200902534

Regulatory Peptides Are Susceptible to Oxidation by Metallic Impurities within Carbon Nanotubes

Adriano Ambrosi[a] and Martin Pumera*[a, b]

Abstract: In this article, we show that the redox properties of the regulatory peptide L-glutathione are affected by the presence of nickel oxide impurities within single-walled carbon nanotubes (SWCNTs). Glutathione is a powerful antioxidant that protects cells from oxidative stress by removing free radicals and peroxides. We show that the L-cysteine moiety in L-glutathione is responsible for the susceptibility to oxidation by metallic impurities present in the carbon nanotubes. These results have great significance for assessing the toxicity of carbon-nanotube materials. The SWCNTs were characterized by Raman spectroscopy, high-resolution X-ray photoelectron spectroscopy, transmission electron microscopy, and energy dispersive X-ray spectroscopy.

Keywords: electrocatalysis · metallic impurities · nanotubes · peptides · redox chemistry

Introduction

Carbon nanotubes (CNTs) are at the forefront of materials research. They have already entered our everyday lives in many ways, such as in gears for sporting equipment.[1] Another wave of carbon-nanotube-based devices and materials, such as batteries, sensors, and polymers filled with CNTs, is expected to enter the market soon.[2] Carbon nanotubes will be produced on a scale in the order of millions of tons per year.[3] Clearly, there is a strong interest in assessing the potential toxicological effects of carbon nanotubes on living organisms; however, the results of toxicological studies to date are inconsistent and, in some cases, even contradictory.[4–6] CNTs are strongly heterogeneous materials containing carbon nanotubes, other forms of carbon (nanographite, amorphous carbon),[7] and residual metal-catalyst impurities.[8,9] The discrepancies in the toxicological data are likely due to the heterogeneous nature of CNTs. The differences have been attributed to the varying amounts of metallic impurities in the CNT samples.[10–13] CNTs are usually grown by arch evaporation or chemical vapor deposition (CVD) synthesis in which metal-catalyst nanoparticles are used (most common are nickel, cobalt, and iron, or a combination of these).[14,15] Although nanocarbon (in its sp^3 and sp^2 forms) is a rather inert material when it interacts with living organisms, the metallic impurities contained in CNTs, which consist of heavy metals such as Fe, Ni, Co, Cu, and Mo, are toxic to living organisms.[16–18] Such metallic impurities can play a significant part in the redox chemistry of biomarkers and metabolic intermediates.[19,20] Carbon nanotubes contain metallic impurities in surprisingly large amounts, which usually range from 1–10 wt%. However, cases in which the amount of metallic impurities is close to 30 wt% of the CNT material are not unusual.[9,21] A wide range of purification methods is available, but these techniques are not very effective. That is, if the purification procedure is successful in reducing the metallic content to 0.5–1 wt%, the resulting CNTs are dubbed "high quality".[22,23] Such removal is not sufficient with regard to participation in the redox reactions of biomarkers. We previously showed that even residual metallic impurities at a level of 0.01 wt% in CNTs strongly participate in the redox chemistry of hydrogen peroxide.[24] It has also been shown that encapsulated Ni and Fe impurities within single-walled carbon nanotubes (SWCNTs) are bioavailable and that they can participate in the redox chemistry of biomolecules in lysosomes.[19,20] Fe-based impurities are responsible for DNA damage by participating in the redox depletion of ascorbate;[19] Ni-based impurities were found to be responsible for disrupting the hydroxylation of transcription factor HIF1-α or inducing gene silencing by binding to heterochromatin.[20] This was despite the fact that the metallic impurities were covered by graphene sheets.[19–21,25] It has been shown that approximately 2–9% of Ni and 1–7% of Fe impurities remain bioavailable even though they are encapsulated within graphene sheets. Such redox availability also extends to multiwalled CNTs (MWCNTs) up to a depth of at least 12 nm.[19–21,25] It has been shown that metallic impurities within CNTs strongly participate in the redox properties of compounds such as hydrazine[26] and halothane.[27] It was also demonstrated that such impurities strongly influence the redox behavior of important biomarkers such as hydrogen peroxide,[28] glucose,[29] and basic amino acids.[30] We recently demonstrated that the issue of metallic impurities is even more complex by showing that, in multicomponent Co/Mo/Fe impurities present in double-walled CNTs, only the Fe component (450 ppm) is redox active towards the reduction of hydrogen peroxide at trace levels,[31] but all components participate in the oxidation of hydrazine.[32] We also showed that bicomponent Ni/Fe residual catalyst impurities within SWCNTs are responsible for the electrochemical oxidation of arginine, in which both Fe and Ni participate, and histidine, in which only Fe participates.[30]

Naturally, one might ask whether the redox chemistry of more complex biomolecules, such as regulatory peptides, is also influenced by the presence of metallic impurities in carbon nanotubes. We selected L-glutathione as a model ex-

[a] Dr. A. Ambrosi, Dr. M. Pumera
Biomaterials Center
National Institute for Materials Science
1-1 Namiki, Tsukuba, Ibaraki 305-0044 (Japan)
Fax: (+81) 29-860-4714
E-mail: PUMERA.Martin@nims.go.jp
martin.pumera@gmail.com

[b] Dr. M. Pumera
International Center for Materials Nanoarchitectonics
National Institute for Materials Science
1-1 Namiki, Tsukuba, Ibaraki 305-0044 (Japan)

ample. Glutathione is an extremely important peptide, present in all living cells (at a concentration of about 5 mM) and in lower concentrations in the blood.[33,34] Glutathione has many functions in living organisms: 1) it is a powerful antioxidant that protects cells from oxidative stress by removing free radicals and peroxides, 2) it acts as a cofactor for a variety of enzymes that require a thiol-reducing equivalent, and 3) higher order cell systems, including redox regulator proteins (metallothioneins, thioredoxins, and peroxidases), are governed by the level of glutathione.[33–35] Thus, it is of great importance to examine the influence of metallic impurities within CNTs on such a vital regulatory biomolecule.

Results and Discussion

We used cyclic voltammetry (CV) to study the oxidation of L-glutathione in the presence of SWCNTs. Figure 1 shows the cyclic voltammetric response towards electrochemical oxidation of glutathione on a SWCNT-modified glassy-carbon (GC) electrode (blue line; for comparison, the CV response of a SWCNT-modified electrode in a blank solution is shown as a dotted blue line). The oxidation of L-glutathione on a SWCNT electrode starts at 40 mV; it exhibits a small shoulder and shows an oxidative peak at about 600 mV. This experiment was followed by a series of experiments to examine the role of SWCNTs (rolled-up sp^2 carbon sheets) and potential metallic impurities in SWCNT samples. We will discuss this series in the next section. Before any further discussion, however, it should be stated that the electrochemistry of CNTs fundamentally resembles that of graphite: heterogeneous electron transfer is fast at the ends of the CNTs and at their defect sites (similar to the edge plane of graphite), whereas pristine CNT walls (similar to the basal plane of graphite) show very low rates of heterogeneous electron transfer.[36–39] Any divergences are linked to the electrochemistry that is caused by impurities within the carbon nanotubes.[2] For this reason, we use an edge-plane pyrolytic graphite (EPPG) electrode as the "reference" material in the following experiments.

We thus examined the amount of edge-plane-like defects in SWCNTs by using Raman spectroscopy and high-resolution X-ray photoelectron spectroscopy (HR-XPS). The Raman spectra of as-received and nitric acid "washed" SWCNTs (Figure 2A, lines a and b, respectively) show two prominent features: a D-band related to sp^3 hybridization and lattice-defect sites at approximately 1350 cm^{-1} and a G-

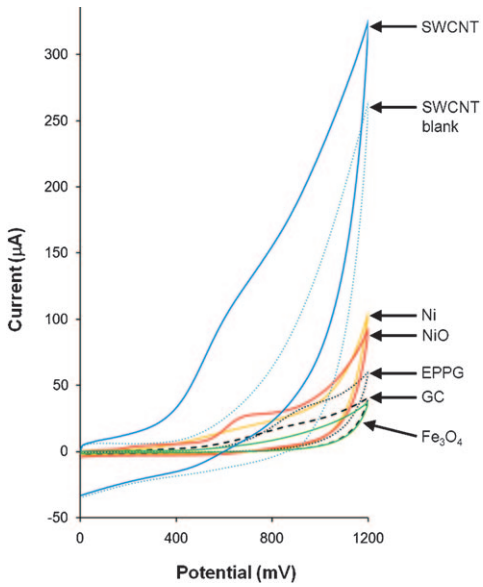

Figure 1. Cyclic voltammograms resulting from electrochemical oxidation of 5 mM L-glutathione at GC electrodes modified with washed SWCNTs (blue line), NiO (red line), Fe_3O_4 (green line), Ni^0 (yellow line), bare EPPG (dotted black line), and GC (dashed black line). Also shown is the response of SWCNTs in the absence of L-glutathione (dotted blue line). Conditions: scan rate: 100 $mV s^{-1}$; background electrolyte: 50 mM phosphate buffer; pH 7.4; reference electrode: Ag/AgCl.

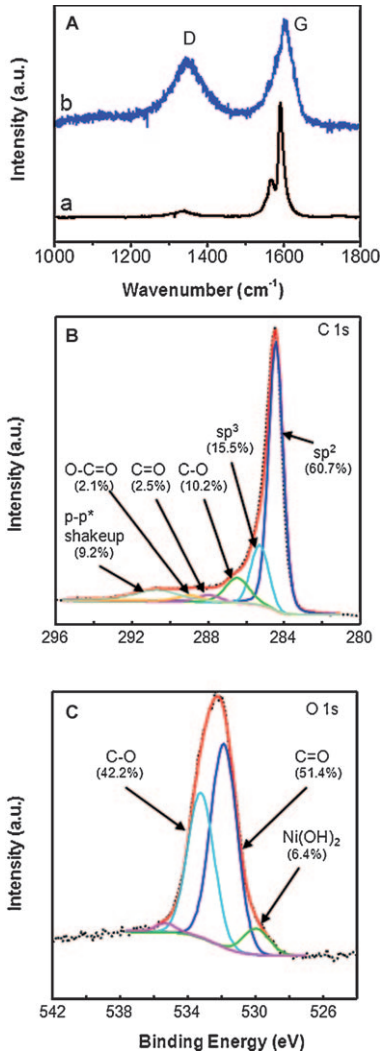

Figure 2. Spectroscopic analysis of defects on SWCNT samples. A) Raman spectra of a) as-received and b) washed SWCNTs (peak high normalized according to the G line). High-resolution XPS spectra of the B) C 1s and C) O 1s signals of washed SWCNTs with appropriate curve fitting.

band related to the doubly degenerate phonon Raman active mode of sp^2 hybridization at 1620 cm^{-1}. It is clear that the D/G ratio increases significantly upon washing of the SWCNTs with nitric acid. The calculated crystallite size[40] (related to defect density) based on the Raman spectra decreases dramatically upon nitric acid washing of the as-received materials, from 392 to 31 nm. HR-XPS spectra of the C 1s core window show one tailing peak at 284.5 eV, with a small shoulder at 291 eV. The C 1s signal can be separated into six quantitative states of carbon stages, namely sp^2-hybridized carbon atoms (at 284.4 eV) of the graphene sheet of a SWCNT, sp^3-hybridized carbon atoms (at 285.2 eV), the alcohol group (C–O; at 286.6 eV), the carbonyl group (C=O; at 288.0 eV), the carboxylic acid group (O–C=O; at 289.2 eV), and the π–π^* shake-up signal (at 290.5 eV), which is typical for sp^2-hybridized carbon atoms (Figure 2B). The fraction of oxygen-containing carbon groups was found to be 14.8%, whereas the fraction of other carbon sp^3 defects was found to be 15.3%. With HR-XPS of the O 1s core oxygen signal (Figure 2C), one can differentiate between the signals from the carboxylic acid/carbonyl groups (O–C=*O* and C=*O*; at 532.2 eV) and the ester groups (C–*O*–C=O; at 533.7 eV). These groups are located at the defect sites. Therefore, it is clear that the XPS and Raman spectroscopy data are consistent.

The amount of oxygen-containing groups on the SWCNT surface is related to the SWCNT-structure defect density, which promotes fast heterogeneous electron transfer.[41–43] The spectroscopic data thus suggest that the number of sites of electroactive defects in the SWCNTs is high and will facilitate electrochemistry much like that of the graphite edge plane.

Bearing this in mind, the following voltammetric experiment involved oxidation of L-glutathione on an EPPG electrode (see Figure 1, black dotted line). The oxidation of L-glutathione on the EPPG electrode starts at about 450 mV and provides a defined peak at 900 mV. There is clearly a large difference between the oxidation behavior of L-glutathione on the SWCNT and EPPG electrodes. As shown below, this difference is due to the presence of metallic impurities within the SWCNTs.

We subjected the SWCNTs to detailed characterization to determine the presence of metallic impurities. The SWCNTs used throughout all of the experiments were purified by the standard procedure of nitric acid washing at 80°C for 36 h, unless stated otherwise. Thermogravimetric analysis of washed SWCNTs showed that they contain about 26.0 wt% of residual inorganic impurities. A subsequent transmission electron microscopy (TEM) study demonstrated that the washed SWCNTs do indeed contain a large number of impurities (Figure 3A). The size of the nanoparticles (NPs) in the SWCNT sample is in the range of 3–20 nm, as determined by observation of more than a hundred NPs. A TEM/energy-dispersive X-ray (EDX) analyzer was used to ascertain the composition of the impurities (Figure 3B). The TEM/EDX results show prominent signals related to Ni Lα, Kα, and Kβ lines. If any other metals are present in the

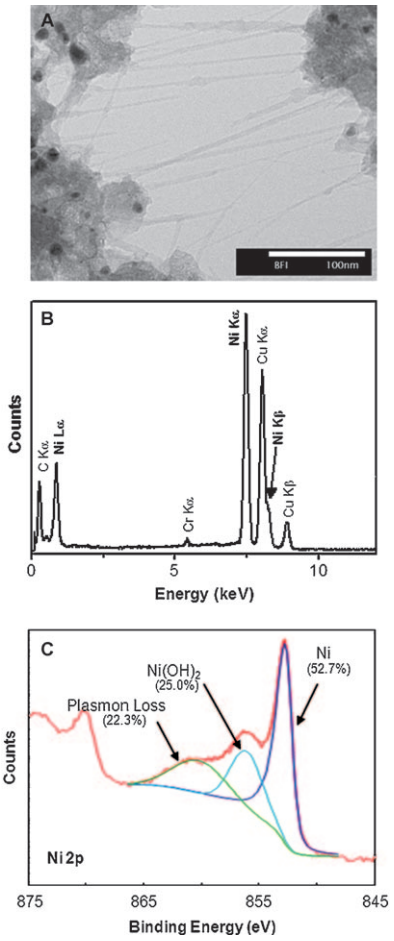

Figure 3. Material analysis of SWCNT samples. A) TEM image of washed SWCNTs containing metallic impurities. B) TEM/EDX spectrum of the impurities featured in (A). C) HR-XPS chemical analysis of the composition of metallic impurities in the SWCNT sample.

SWCNT sample, they are below the detection limit of the TEM/EDX analyzer. It should be noted that the Cu- and Cr-related lines originate from the specimen holder. Inductively coupled plasma atomic emission spectroscopy (ICP-AES) analysis of residual impurities showed that the content of Ni was 22.3 wt% and that of Fe was 0.1 wt%. High-resolution XPS was utilized to obtain information on the chemical composition of Ni impurities. HR-XPS spectra exhibit two separate peaks resulting from $Ni(OH)_2$ at a binding energy of (855.7 ± 0.4) eV and Ni^0 at a binding energy of (852.7 ± 0.2) eV (Figure 3C). In addition, it is possible to observe the signal of $Ni(OH)_2$ in the O 1s core spectrum (Figure 2C). The concentration of Fe is too low to be detected by XPS, which is a surface-sensitive technique.

Based on the material characterization data, we modified the surface of the GC electrode with NiO, Ni, and F_3O_4 nanoparticles and compared the response towards the oxidation of L-glutathione with those of the SWCNT and EPPG electrodes. Figure 1 illustrates that the oxidation of L-glutathione on the NiO-NP-modified electrode (red line) starts at 250 mV, reaches a first maximum at 260 mV, gives another

redox wave that starts at 420 mV, and exhibits an oxidative peak at 650 mV. L-Glutathione does not exhibit any oxidation with the Fe_3O_4-NP-modified electrode (green line). The Ni^0-NP-modified GC electrode (yellow line) leads to a slight increase in oxidation at 240 mV, but it does not differ qualitatively from the signal with a bare GC electrode (dashed black line). Thus, these two electrodes do not possess any electrocatalytic effect. We also performed control experiments involving all relevant electrodes and a blank solution containing only buffer without the presence of L-glutathione, and we observed no voltammetric signal (data not shown). Comparisons between the voltammetric behaviors of the SWCNTs and the NiO-, Ni-, Fe_3O_4-, and EPPG-modified electrodes led us to the conclusion that the NiO nanoparticles within the SWCNTs are responsible for the electrocatalytic behavior of the SWCNTs towards the oxidation of L-glutathione. It should be added that even a small amount of electroactive nanoparticles at very small random array coverage may exhibit behavior analogous to that of the corresponding macroelectrode, as has been shown theoretically and experimentally.[44–46] This is due to heavily overlapping diffusion layers of such nanoparticles.

We next turned to investigate the reason for the oxidation of L-glutathione in our system. L-glutathione is a tripeptide consisting of L-cysteine, L-glutamic acid, and glycine. We performed voltammetric experiments involving the oxidation of these amino acids on SWCNT, NiO, Ni^0, Fe_3O_4, and EPPG electrodes, as shown in Figure 4. L-Cysteine (Figure 4A) exhibits oxidation on SWCNT-modified electrodes, with the oxidative current starting at 25 mV and reaching an oxidative peak at 550 mV (Figure 4A, blue line). The oxidation on the EPPG electrode starts at 250 mV and reaches an oxidative peak at 750 mV (Figure 4A, black dotted line). The oxidation of L-cysteine at the NiO electrode starts at 50 mV, reaches a first oxidative wave at 260 mV, starts a second wave at around 420 mV, and reaches a second oxidative peak at 640 mV (Figure 4A, red line). L-Cysteine exhibits its oxidation currents at the Ni^0- and Fe_3O_4-NP-modified electrodes (Figure 4A, yellow and green lines, respectively) with a peak potential of 750 mV. However, this oxidation potential is the same as the potential at which the L-cysteine is oxidized on the EPPG and GC electrodes (750 mV; Figure 4A, dotted and dashed black lines, respectively). Thus, these NPs do not create any electrocatalytic effect towards the oxidation of L-cysteine. Thus, the electrocatalytic behavior of SWCNTs towards L-cysteine originates in NiO-based impurities. We also recorded blank voltammograms for all of the electrode types and components in question, but no voltammetric signals were observed (data not shown). L-Glutamic acid and glycine were also subjected to voltammetric oxidation (Figure 4B and C, respectively), but none of the voltammetric signals were different from those of the blank solutions recorded. A comparison of the behavior of L-cysteine on the SWCNT electrode with that on the NiO-modified electrodes led us to conclude that L-cysteine is responsible for the redox behavior of L-glutathione in the above-mentioned experiments. The oxidation process can be described by Equation (1),[47] in which RSH is the L-glutathione moiety.

$$2RSH - 2e^- - 2H^+ \xrightarrow{NiO} RSSR \quad (1)$$

Such a reaction is catalyzed by NiO; at different surfaces such as Pt,[48] Fe_3O_4, Ni, GC, and EPPG surfaces, it takes place at significantly higher potentials.

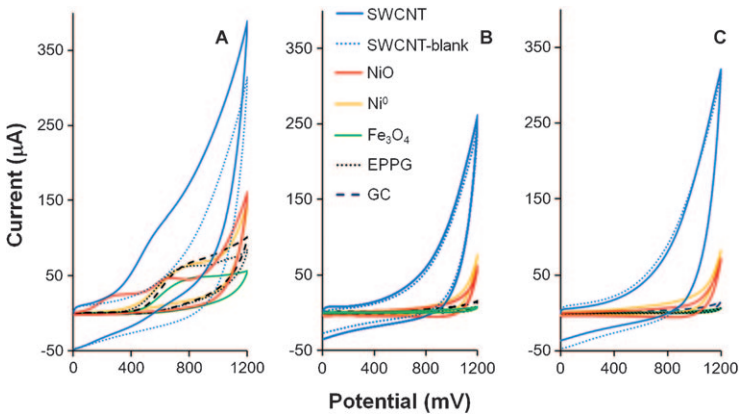

Figure 4. Cyclic voltammograms resulting from electrochemical oxidation of A) L-cysteine, B) L-glutamic acid, and C) glycine (all 5 mM) at GC electrodes modified with washed SWCNTs (blue line), NiO (red line), Fe_3O_4 (green line), Ni^0 (yellow line), bare EPPG (dotted black line), and GC (dashed black line). Also shown is the response of SWCNTs in the absence of L-glutathione (dotted blue line). Conditions: scan rate: 100 mV s^{-1}; background electrolyte: 50 mM phosphate buffer; pH 7.4; reference electrode: Ag/AgCl.

Conclusions

We have clearly demonstrated that NiO metallic impurities in SWCNTs strongly participate in the redox behavior of an important regulatory peptide, L-glutathione, and that they are responsible for the electrocatalytic oxidation of L-glutathione. This is the first example of such a direct influence of metallic impurities on the oxidation of peptides. This influence has important biomedical implications regarding the toxicity of carbon nanotubes. Other peptides containing cysteine in its reduced form are also expected to be subject to oxidation in the presence of NiO impurities in CNTs. An investigation of the influence of metallic impurities on other peptides and proteins and their biochemical pathways is currently under way.

Experimental Section

Materials: Single-walled carbon nanotubes (diameter × length: 1.2–1.5 nm × 2–5 μm; three different batches contained SWCNTs of similar quality); *N*,*N*-dimethyl formamide (DMF), nitric acid (the highest purity commercially available, super-special purity according to Sigma–Aldrich), potassium phosphate dibasic, sodium phosphate monobasic, nickel(II) oxide nanoparticles (diameter < 50 nm), iron(II, III) oxide (diameter < 50 nm), nickel (Ni^0) NPs (diameter < 50 nm), L-glutathione, L-cysteine,

L-glutamic acid, and glycine were purchased from Sigma–Aldrich (Japan). Edge-plane pyrolytic graphite (EPPG) and glassy-carbon (GC) electrodes (diameter = 3 mm) were obtained from Autolab (Japan).

Apparatus: A JEM 2100F field-emission transmission electron microscope (JEOL, Japan) operating at 200 kV was used to acquire TEM images in a scanning TEM mode (spot size of 0.7 nm). TEM/EDX spectra were collected by using the JEM 2100F microscope equipped with an energy-dispersive X-ray spectrometer with an ultrathin window (JEOL). X-ray photoelectron spectroscopy (XPS) was performed with a PHI Quantera SXM (ULVAC-PHI, Japan) with a monochromatic Al Kα X-ray source. The analysis area was defined by a 1.5×0.1 mm scanned beam at a beam energy of 20 kV and 100 W; the photoelectron take-off angle was set at 45 degrees. For high-resolution XPS scans, the pass energy was set at 112 eV, with steps of 0.1 eV. An electron beam of 20 μA at 1.4 eV and an argon ion beam of 30 nA at 7 eV were irradiated on the sample for charge neutralization. The energies of all spectra were shifted by correcting the C 1s peak as sp^2 at 284.5 eV for energy calibration. Raman spectra were obtained by using a T64000 Raman spectrometer (Horiba Jobin Yvon Ltd., Japan) with excitation from an argon ion laser beam ($\lambda = 514.5$ nm) employing backscattering geometry. All voltammetric experiments were performed by using an Autolab 302 electrochemical analyzer (Eco Chemie, The Netherlands) connected to a personal computer and controlled by General Purpose Electrochemical Systems Version 4.9 software (Eco Chemie). Electrochemical experiments were performed in a 5 mL voltammetric cell at room temperature (25°C) by using a three-electrode configuration. A platinum electrode served as an auxiliary electrode; an Ag/AgCl electrode served as a reference electrode. All electrochemical potentials in this paper are stated versus Ag/AgCl reference electrode.

Procedures: As-received carbon-nanotube materials were stirred in concentrated nitric acid (6 M) for 36 h at 80°C. The acid/SWCNT mixture was subsequently washed with distilled water and centrifuged several times until the aqueous solution reached a neutral pH value. The washed carbon nanotubes were then filtered through a 0.2 μm membrane (Nuclepore Track-Etched Membrane, Whatman, UK) under vacuum. Carbon nanotubes treated like this are referred to in the text as "washed". The EPPG- and GC-electrode surfaces were renewed by polishing with 0.05 μm alumina particles on a cloth. For the electrochemical measurements, the carbon nanotubes were cast onto a GC-electrode surface. The nanotubes were first dispersed in DMF at a concentration of 1 mg mL^{-1}. The suspension was then placed into an ultrasound bath for 5 min, after which time a portion of the suspension (5 μL) was pipetted onto the GC-electrode surface. The suspension was allowed to evaporate at room temperature, to create a randomly distributed SWCNT film on the GC-electrode surface. Nanoparticle-modified GC electrodes were prepared in a similar manner by dispersing nanoparticles in DMF (1 mg mL^{-1}) and subsequent deposition of the dispersed NPs (5 μL) on the GC surface. Cyclic voltammetry experiments were performed at a scan rate of 100 mV s^{-1} by using 50 mM phosphate buffer (pH 7.4). The SWCNT samples were powder-like and were therefore coated on carbon tape for XPS measurement. For TEM measurements, a 0.5 mg mL^{-1} suspension of CNTs (1 μL) was dropped on a copper TEM grid and allowed to dry in air.

Calculation: The crystallite size (L_a) of the sp^2 lattice was calculated according to Equation (2),[40] in which λ_{laser} is the laser wavelength in nm units, I_G is the intensity of the Raman G-band and I_D is the intensity of the Raman D-band.

$$L_a = 2.4 \times 10^{-10} \times \lambda_{laser}^4 \times \frac{I_G}{I_D} \quad (2)$$

Acknowledgements

This work was supported in part by the World Premier International Research Center (WPI) Initiative on Materials Nanoarchitectonics, MEXT, Japan. The author is indebted to the Materials Analysis Station (NIMS) for ICP-AES and XPS measurements. Frontispiece photography is courtesy of Květa Pumerová.

[1] *Anonymous, Nano Magazine* **2008**, *9*, 14.
[2] M. Pumera, *Chem. Eur. J.* **2009**, *15*, 4970.
[3] A. M. Thayer, *Chem. Eng. News* **2007**, *85*, 29.
[4] J. M. Wörle-Knirsch, K. Pulskamp, H. F. Krug, *Nano Lett.* **2006**, *6*, 1261.
[5] D. Zhu, W. Chang, L. Dai, Y. Hong, *Nano Lett.* **2007**, *7*, 3592.
[6] S. K. Smart, A. I. Cassady, G. D. Lu, D. J. Martin, *Carbon* **2006**, *44*, 1034.
[7] M. E. Itkis, D. E. Perea, R. Jung, S. Niyogi, R. C. Haddon, *J. Am. Chem. Soc.* **2005**, *127*, 3439.
[8] T. Kolodiazhnyi, M. Pumera, *Small* **2008**, *4*, 1476.
[9] G. Charron, S. Mazerat, M. Erdogan, A. Gloter, A. Filoramo, J. Cambedouzou, P. Launois, E. Rivière, W. Wernsdorfer, J.-P. Bourgoin, T. Mallah, *New J. Chem.* **2009**, *33*, 1211.
[10] A. Nimmagadda, K. Thurston, M. U. Nollert, P. S. McFetridge, *J. Biomed. Mater. Res.* **2006**, *76*, 614.
[11] V. E. Kagan, Y. Y. Tyurina, V. A. Tyurin, N. V. Konduru, A. I. Potapovich, A. N. Osipov, E. R. Kisin, D. Schwegler-Berry, R. Mercer, V Castranova, A. A. Shvedova, *Toxicol. Lett.* **2006**, *165*, 88.
[12] A. E. Porter, M. Gass, K. Muller, J. N. Skepper, P. A. Midgley, M. Welland, *Nat. Nanotechnol.* **2007**, *2*, 713.
[13] C.-W. Lam, J. T. James, R. McCluskey, A. Holian, R. L. Hunter, *Toxicity of Carbon Nanotubes and its Implications for Occupational and Environmental Health* (Ed.: C. S. S. R. Kumar), Wiley-WCH, Weinheim, **2007**, p. 130.
[14] P. J. F. Harris, *Carbon* **2007**, *45*, 229.
[15] D. Takagi, Y. Homma, H. Hibino, S. Suzuki, Y. Kobayashi, *Nano Lett.* **2006**, *6*, 2642.
[16] M. Horie, K. Nishio, K. Fujita, H. Kato, A. Nakamura, S. Kinugasa, S. Endoh, A. Miyauchi, K. Yamamoto, H. Murayama, E. Niki, H. Iwahashi, Y. Yoshida, J. Nakanishi, *Chem. Res. Toxicol.* **2009**, *22*, 1415.
[17] M. Horie, K. Nishio, K. Fujita, S. Endoh, A. Miyauchi, Y. Saito, H. Iwahashi, K. Yamamoto, H. Murayama, H. Nakano, N. Nanashima, E. Niki, Y. Yoshida, *Chem. Res. Toxicol.* **2009**, *22*, 543.
[18] H. L. Karlsson, P. Cronholm, J. Gustafsson, L. Möller, *Chem. Res. Toxicol.* **2008**, *21*, 1726.
[19] X. Liu, V. Gurel, D. Morris, D. Murray, A. Zhitkovich, A. B. Kane, R. H. Hurt, *Adv. Mater.* **2007**, *19*, 2790.
[20] L. Guo, D. G. Morris, X. Liu, C. Vaslet, R. H. Hurt, A. B. Kane, *Chem. Mater.* **2007**, *19*, 3472.
[21] M. Pumera, *Langmuir* **2007**, *23*, 6453.
[22] P.-X. Hou, C. Liu, H.-M. Cheng, *Carbon* **2008**, *46*, 2003.
[23] B. Ballesteros, G. Tobias, L. Shao, E. Pellicer, J. Nogues, E. Mendoza, M. L. H. Green, *Small* **2008**, *4*, 1501.
[24] M. Pumera, Y. Miyahara, *Nanoscale* **2009**, *1*, 260.
[25] X. Liu, L. Guo, D. Morris, A. B. Kane, R. H. Hurt, *Carbon* **2008**, *46*, 489.
[26] C. E. Banks, A. Crossley, C. Salter, S. J. Wilkins, R. G. Compton, *Angew. Chem.* **2006**, *118*, 2595; *Angew. Chem. Int. Ed.* **2006**, *45*, 2533.
[27] X. Dai, G. G. Wildgoose, R. G. Compton, *Analyst* **2006**, *131*, 901.
[28] B. Šljukić, C. E. Banks, R. G. Compton, *Nano Lett.* **2006**, *6*, 1556.
[29] C. Batchelor-McAuley, G. G. Wildgoose, R. G. Compton, L. Shao, M. L. H. Green, *Sens. Actuators B* **2008**, *132*, 356.
[30] M. Pumera, H. Iwai, Y. Miyahara, *ChemPhysChem* **2009**, *10*, 1770.
[31] M. Pumera, H. Iwai, *Chem. Asian J.* **2009**, *4*, 554.
[32] M. Pumera, H. Iwai, *J. Phys. Chem. C* **2009**, *113*, 4401.
[33] *Glutathione: Chemical, Biochemical, and Medical Aspects* (Eds.: D. Dolphin, R. Poulson, O. Avramovic), Wiley, New York, **1989**.
[34] J. Vina, *Glutathione: Metabolism and Physiological Functions*, CRC, Boca Raton, **2000**.
[35] O. N. Oktyabrsky, G. V. Smirnovam, N. G. Muzika, *Free Radical Biol. Med.* **2001**, *31*, 250.
[36] R. R. Moore, C. E. Banks, R. G. Compton, *Anal. Chem.* **2004**, *76*, 2677.
[37] T. J. Davies, M. E. Hyde, R. G. Compton, *Angew. Chem.* **2005**, *117*, 5251; *Angew. Chem. Int. Ed.* **2005**, *44*, 5121.

[38] A. F. Holloway, G. G. Wildgoose, R. G. Compton, L. Shao, M. L. H. Green, *J. Solid State Electrochem.* **2008**, *12*, 1337.
[39] M. Pumera, T. Sasaki, H. Iwai, *Chem. Asian J.* **2008**, *3*, 2046.
[40] L. Cancado, K. Takai, T. Enoki, M. Endo, Y. A. Kim, H. Mizusaki, A. Jorio, L. N. Coelho, R. Magalhaes-Paniago, M. A. Pimenta, *Appl. Phys. Lett.* **2006**, *88*, 163106.
[41] M. Pumera, B. Šmíd, K. Veltruská, *J. Nanosci. Nanotechnol.* **2009**, *9*, 2671.
[42] A. Chou, T. Böcking, N. K. Singh, J. J. Gooding, *Chem. Commun.* **2005**, 842.
[43] M. Pumera, *Chem. Asian J.* **2009**, *4*, 250.
[44] T. J. Davies, C. E. Banks, R. G. Compton, *J. Solid State Electrochem.* **2005**, *9*, 797.
[45] T. J. Davies, R. G. Compton, *J. Electroanal. Chem.* **2005**, *585*, 63.
[46] X. Dai, G. G. Wildgoose, C. Salter, A. Crossley, R. G. Compton, *Anal. Chem.* **2006**, *78*, 6102.
[47] O. Nekrassova, G. D. Allen, N. S. Lawrence, L. Jiang, T. G. J. Jones, R. G. Compton, *Electroanalysis* **2002**, *14*, 1464.
[48] D. Giovanelli, N. S. Lawrence, L. Jiang, T. G. J. Jones, R. G. Compton, *Sens. Actuators B* **2003**, *88*, 320.

Received: September 15, 2009
Published online: January 11, 2010

